Effect of light-collection geometry on reconstruction errors in Abel inversions

Kevin T. Walsh, Joseph Fielding, and Marshall B. Long

Department of Mechanical Engineering, Yale University, New Haven, Connecticut 06520-8284

Received November 12, 1999

The Abel inversion, used to reconstruct axisymmetric radial profiles from line-of-sight intensity measurements, is increasingly used to make spatially resolved combustion measurements. An Abel deconvolution is valid only when incoming rays are parallel, whereas most practical optical setups used for emission imaging consist of single-lens and multilens systems that collect light in a cone, over a nonzero solid angle. A ray-tracing simulation was performed to aid in understanding how optical collection geometry affects measured intensity signals and the resultant reconstructed emissivity profiles. Simulation results are compared with emission tomography measurements performed on an axisymmetric laminar diffusion flame. © 2000 Optical Society of America

OCIS codes: 120.1740, 110.6960.

Spatially resolved measurements of combustion parameters, such as species concentration, temperature, and soot volume fraction, are important in fundamental flame research.[1] Unfortunately, some combustion measurement techniques, such as emission and absorption, collect signal along the entire line of sight. Tomographic techniques are therefore needed for reconstruction of the two- or three-dimensional quantity under investigation. In particular, an Abel inversion can be used to reconstruct a cylindrically symmetric distribution from line-of-sight intensity measurements.[2] This deconvolution is valid only when the measured signal is collected along infinitely thin, perfectly parallel rays.

Absorption measurements with collimated laser sources conform closely to the parallel-ray assumption, as do traditional single-point emission measurements involving spatial filters and simple light detectors. In emission imaging, however, these light-collection criteria can only be approximated in a realizable measurement system. The single-lens and multilens optics used in practical measurements collect nonparallel rays in a cone, over a nonzero solid angle. To the best of our knowledge, no one has investigated how these effects influence the measured intensity profile and the resultant radial distribution computed with an Abel inversion. These effects could be important for interpreting recent measurements of both relative and absolute radical concentrations performed with emission tomography.[3–5] For relative concentration measurements, the chosen collection optics may widen or distort the measured intensity profile relative to parallel ray collection. Determining absolute concentrations could potentially be problematic as well, inasmuch as collection over a cone results in higher peak signals than assumed by parallel ray collection. The relative scale factor is sensitive to the geometry of both the distribution that is being measured and the collection optics.

A ray-tracing simulation was performed to quantify some of these issues. The results are compared with CH* chemiluminescence measurements in an axisymmetric laminar diffusion flame.[4] CH* exists in a thin, high-temperature region and therefore serves as a marker of the flame front.[6] Integrated CH* emission is imaged over the entire flame, and one-dimensional intensity profiles are extracted at various axial heights for comparison with the predictions of these simulations. Because these measurements had a high signal-to-noise ratio, no smoothing was required before the Abel inversion was performed.

One can determine an axisymmetric emissivity distribution $F(r)$ by measuring the line-of-sight integrated signal at a single angle and performing an Abel deconvolution, as is shown graphically in Fig. 1 and described here. When infinitely thin, parallel rays are collected across the entirety of $F(r)$, the line-of-sight integrated intensity profile $I(y)$ is given by

$$I(y) = \int_{-\infty}^{\infty} F[(x^2 + y^2)^{1/2}]\mathrm{d}x\,.$$

The emissivity $F(r)$ can be recovered from projection data with the use of the Abel inversion, which is written analytically as

$$F(r) = -\frac{1}{\pi}\int_{r}^{\infty} \frac{I'(y)}{(y^2 - r^2)^{1/2}}\,\mathrm{d}y\,,$$

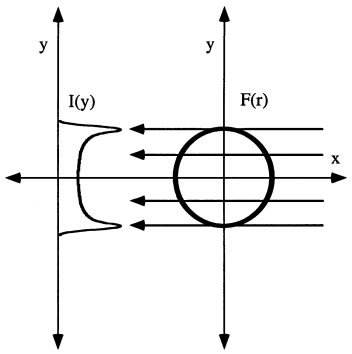

Fig. 1. Illustration of projection measurement with parallel beam collection.

0146-9592/00/070457-03$15.00/0

where $I'(y) = dI/dy$. Several implementation procedures to perform this inversion are available. Here an algorithm that is equivalent to a two-point Abel deconvolution is utilized.[7]

A ray-tracing algorithm was developed to simulate measured integrated intensity profiles. The coordinate system used is diagrammed in Fig. 2. The function $F(r)$, centered at $(x = r_i, y = 0)$, is represented on a pixelated grid. The pixel width is dx, and the imaged region is a square of side length $2r_i$. A lens of diameter d is placed a distance f_o from the near edge of the imaged region. In two dimensions, the integrated intensity from the point (x_0, y_0) is collected from the two triangular regions, labeled $R(x_0, y_0)$, bounded by the rays shown in the diagram. The total integrated intensity at y_0 is the sum of the signals collected as x_0 is varied. This is expressed mathematically as

$$\text{2D:} I(y_0) = \sum_{x_0=0}^{2r_i} \sum_{x=0}^{2r_i} \sum_{y \in R(x_0, y_0)} F\{[(x - r_i)^2 + y^2]^{1/2}\},$$

where 2D means two dimensions. The equations of the two lines that define $R(x_0, y_0)$ are shown in Fig. 2. Note that, in the limit of $f_o \to \infty$, this region collapses to the line $y = y_0$, and parallel ray collection is recovered. This was confirmed in the simulation.

Extending the simulation to three dimensions requires the inclusion of all signals collected in a three-dimensional cone. We form this cone by rotating the triangular regions $R(x_0, y_0)$ about the chief ray, which goes between $(-f_o, 0)$ and (x_0, y_0). To perform this three-dimensional intensity collection, we assume that the measured distribution is a stack of planes with thickness dx and emissivity $F(r)$. Contributions from adjacent planes are added by additional two-dimensional summations over regions defined by the intersection of the collection cone with the appropriate plane.

The magnitudes of the simulated intensity distributions from the cone-collected signals and the parallel ray signals are different because of geometric distortions as well as changes in the solid angle of collection. To account for this, a laser calibration method, which is used to calibrate actual emission measurements,[8] was simulated with the same program. Signals collected from a 300-μm-thick laser beam were simulated, and a scale factor was found between the parallel ray–collected and the cone-collected signals, which varied as the simulation parameters (f_o, d, dx, and r_i) were changed. This scale factor was computed in each case to permit direct comparison of simulated parallel ray–collected and cone-collected signals.

For CH* chemiluminescence imaging measurements reported previously,[4] light was collected with a single lens of diameter $d = 22$ mm a distance $f_0 = 500$ mm away from the edge of the imaged region. The depth of field was determined to be grater than the flame width, and the measured pixel size (dx) was 68 μm. To match measured intensity profiles, $F(r)$ was modeled as a Lorentzian on one side and as a step function on the other. The geometrical parameters used in the flame measurements were used for our simulation, with the peak location and width of $F(r)$ varied as free parameters to agree best with measured data.

The simulated and measured signal intensities are shown on the left-hand side of Fig. 3, along with the parallel ray signal. The simulated distribution has a peak at $r = 3.9$ mm; r_i was 12 mm. The measured and simulated signals agree quite well. Both are shorter and wider than the parallel ray profile, with higher magnitudes along the centerline.

The simulated signals can now be Abel inverted, allowing the calculated $F(r)$ to be compared with the emissivity reconstructed from parallel rays, as shown on the right-hand side of Fig. 3. The actual $F(r)$ used in the simulation, not shown, is nearly

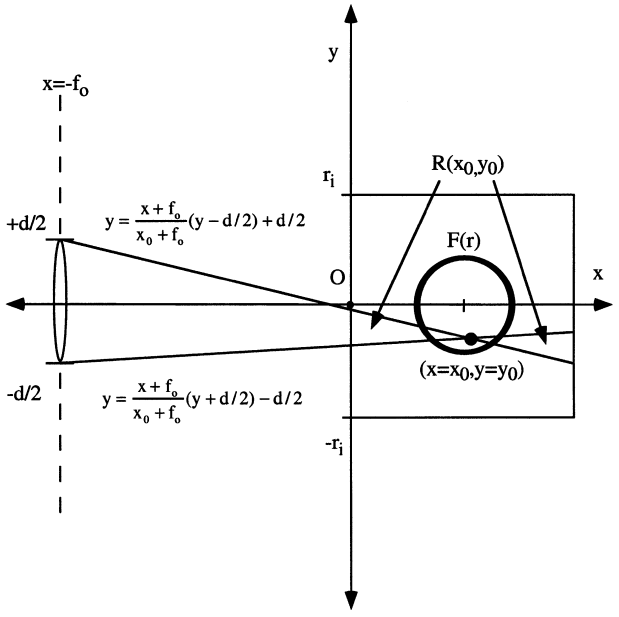

Fig. 2. Coordinate system used for signal collection simulation.

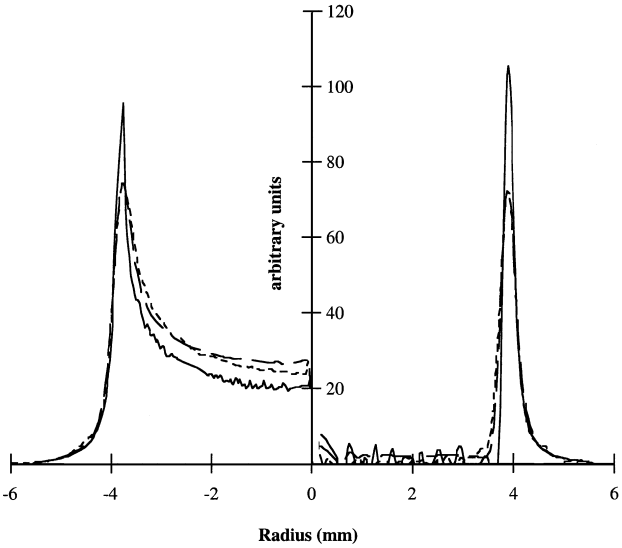

Fig. 3. Left, integrated intensity signal from experimental data (short-dashed curve), simulated three-dimensional optical collection (long-dashed curve), and simulated parallel ray collection (solid curve). Right, Abel-inverted emissivity profiles of the curves shown at the left.

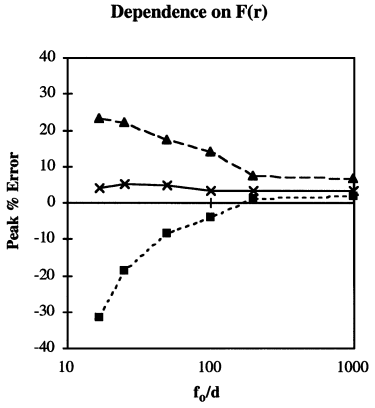

Fig. 4. Peak reconstruction errors, as a function of f_o/d for three radial distributions: crosses, Gaussian; triangles, top-hat; squares, CH*.

indistinguishable from the reconstructed parallel ray profile. The integrated signal from cones with a finite solid angle gives a computed emissivity profile that is shorter and wider than the parallel ray profile. There is also a 1-pixel difference in the location of the peak. After the Abel inversion is performed, there exists low-magnitude residual noise from the centerline to where the distribution peaks, which is an artifact of all Abel inversion algorithms.

For the chemiluminescence measurements of Ref. 4, the spatial resolution is estimated to be 2 pixels, or $\sim$140 μm. Therefore the 1-pixel difference in peak location and the 2-pixel difference in the full width at half-maximum between the reconstructed and the actual $F(r)$ fall within the experimental uncertainty. These CH* emissivity profiles can therefore be used to determine flame shape. The 30% inaccuracy in peak signal, however, is significant and needs to be combined with other experimental uncertainties for access to the accuracy in the measured peak CH* concentration.

As a general trend, errors in the reconstructed profiles tend to diminish as f_o/d approaches infinity and collected rays become more nearly parallel. However, the magnitude of these errors depends on the distribution being measured, $F(r)$, as well as on the optical collection geometry. This dependence is shown in Fig. 4, where the peak percent error is plotted as a function of f_o/d for three simulated distributions that were similar in spatial extent. These calculations were done with f_o = 1000 mm, dx = 0.068 mm, and r_i = 12 mm. For a Gaussian profile, reconstruction errors are small over a wide range of collection geometries. However, for a top-hat profile of radius 5 mm, the reconstructed peak values are significantly overpredicted. As was noted above, the peak of the narrow CH* distribution is underpredicted. This different behavior in identical collection geometries suggests that detailed, distribution-specific calculations are requirements for quantifying measurement errors and interpreting measured signals in emission tomography applications for which parallel ray collection is required.

The authors thank Philip Varghese of the University of Texas at Austin for suggesting this research. The support of NASA under grant NAG2-1939 is gratefully acknowledged. M. B. Long's e-mail address is marshall.long@yale.edu.

References

1. A. C. Eckbreth, *Laser Diagnostics for Combustion Temperature and Species*, 2nd ed., Vol. 3 of Combustion Science and Technology Book Series (Gordon & Breach, Amsterdam, 1996).
2. B. J. Hughley and D. A. Santavicca, Combust. Sci. Technol. **29,** 167 (1982).
3. A. J. Marchese, F. L. Dryer, M. Vedha-Nayagam, and R. Colantonio, in *Twenty-Sixth Symposium (International) on Combustion* (Combustion Institute, Pittsburgh, Pa., 1996), p. 1219.
4. K. T. Walsh, M. B. Long, M. A. Tanoff, and M. D. Smooke, in *Twenty-Seventh Symposium (International) on Combustion* (Combustion Institute, Pittsburgh, Pa., 1998), p. 615.
5. J. Luque, W. Juchmann, E. A. Brinkman, and J. B. Jeffries, J. Vac. Sci. Technol. A **16,** 397 (1998).
6. M. D. Smooke, Y. Xu, R. M. Zurn, P. Lin, J. H. Frank, and M. B. Long, in *Twenty-Fourth Symposium (International) on Combustion* (Combustion Institute, Pittsburgh, Pa., 1992), p. 813.
7. C. J. Dasch, Appl. Opt. **31,** 1146 (1994).
8. J. Luque and D. R. Crosley, Appl. Phys. B **63,** 91 (1996).
9. H. M. Hertz and G. W. Faris, Opt. Lett. **13,** 351 (1988).